

Processing and properties of porous piezoelectric materials with high hydrostatic figures of merit

C.R. Bowen*, A. Perry, A.C.F. Lewis, H. Kara

Material Research Centre, Department of Engineering and Applied Science, University of Bath, Bath BA2 7AY, UK

Abstract

Porous piezoelectric materials are of interest for applications such as low frequency hydrophones. This is due to their high hydrostatic figures of merit and low sound velocity, which leads to reduced acoustic impedance and enhanced coupling with water or biological tissue. A wide variety of methods are available to produce porous structures such as using reticulated polymer foams or volatile additives which are burnt out during the sintering process (e.g. polymer spheres). Each processing technique and additive produces its own distinctive microstructure, particularly in terms of pore size, morphology and porosity volume fraction. The aim of this paper is to manufacture a variety of porous microstructures and relate the structures to measured hydrostatic figures of merit.

© 2003 Elsevier Ltd. All rights reserved.

Keywords: Fillers; Piezoelectric properties; Porosity; PZT; Hydrostatic strain

1. Introduction

The use of piezoelectric ceramics such as lead zirconate titanate (PZT) in composite form has been widely studied since the work of Newnham.¹ A two-digit number, whereby the first number corresponds to the connectivity of the active phase (PZT) and the second number corresponds to the connectivity of the passive phase (polymer or air) classifies these ‘piezocomposites’. Porous piezoelectric materials can be classified as ‘3–3’ piezocomposites when both the piezoelectric phase and porosity are interconnected, as occurs in porous materials with a high degree of open porosity. These materials are of interest as they have a number of possible advantages over dense monolithic piezoceramics, particularly for applications such as low frequency hydrophones. Firstly, the difference in acoustic impedance of the piezoelectric and the ambient medium (such as air or water) determines the reflection and transmission of sound energy at the interface.² The closer the impedances are to each other, the less sound energy is reflected at the interface. This ‘impedance matching’ can be achieved by incorporating porosity into the piezo-

ceramic and reducing the sound velocity and impedance to values closer to water or air. Secondly, an increase in the amount of porosity leads to a decrease in the transverse piezoelectric coefficient ($-d_{31}$) relative to the longitudinal piezoelectric coefficient (d_{33}).³ This produces an increase in the *hydrostatic strain coefficient*, d_h ($=d_{33} + 2d_{31}$), so that higher electrical charges are generated per unit hydrostatic force. Hydrostatic conditions arise in hydrophones when attempting to detect low frequency signals as the acoustic wavelengths are larger than the material/device and the device therefore lies within individual compressions and rarefaction of the acoustic signal.⁴ Finally, the reduction in permittivity (ϵ_{33}) of the porous material as piezoelectric ceramic is replaced by air increases the *piezoelectric voltage coefficients* (g_{ij}), which is a measure of the electric field generated per unit stress. If we consider the *hydrostatic voltage coefficient*, $g_h = d_h/\epsilon_{33}$ which is a measure of electric field generated per unit hydrostatic stress, the improved d_h and reduced ϵ_{33} of porous piezoceramics leads to significant improvements in the figure of merit when compared to dense monolithic material.⁴ The increase in g_h implies an increase in the sensitivity of a hydrophone, which is generally a measure of voltage generated per unit stress.⁵ It has also been reported that porous materials potentially offer a high signal to noise ratio for a given volume of material due to the increased

* Corresponding author. Tel.: +44-1255-323660; fax: +44-1225-826098.

E-mail address: c.r.bowen@bath.ac.uk (C.R. Bowen).

hydrostatic figure of merit (HFOM), which is the product $d_h g_h$.^{5,6}

Modelling of 3–3 structures has shown that the figures of merit d_h , g_h and $d_h g_h$ are a strong function of porosity volume fraction and the optimum level of porosity depends on the figure of merit that needs to be maximised.⁷ In order to manufacture porous structures of particular pore volume fraction, size and morphology a variety of methods have been employed. For example, Creedon et al.³ has used polymer foams which are coated with a piezoceramic, Skinner et al. used a coral replamine process,¹ Shrout and Rittenmyer used volatile plastic spheres,⁸ Geis et al. used an aerogel process² and Craciun et al. used tape casting with a cellulose derivative.⁹ Each process produces its own distinctive microstructure, pore size and morphology and, in addition, different techniques are only able to produce a specific range of porosity. For example, foam techniques are only suitable for processing high porosity volume fraction materials (>90%) while the use of volatile additives is suitable for lower levels of porosity (<60%) as a high volatile content often results in deformation and destruction of the green body during the burn out cycle. As the porosity volume fraction changes there can also be different fractions of closed and open porosity, changing the connectivity from ‘3–3’ to a ‘3–0’ type.¹⁰ These factors make it difficult to experimentally examine the complete range of porosity for a given pore size and morphology, which is often considered when modelling piezocomposite structures.^{7,8,11} The aim of this paper is to manufacture various types of microstructure and relate the structures to the measured piezoelectric parameters. This will provide an improved understanding of the manufacturing methods and related piezoelectric properties.

2. Experimental

For all the porous materials manufactured in this work, PZT-5H from Morgan Electroceramics was used as the base piezoceramic, which is a soft lead zirconate titanate widely used for low frequency actuators and sensors. Typical properties of the dense material are a density of 7500 kgm^{-3} , $d_{33} = 590 \text{ pCn}^{-1}$, $d_{31} = -270 \text{ pCn}^{-1}$ with a relative permittivity at constant stress of 3500. The material has a high d_{33} but the high negative value of d_{31} and high permittivity results in low d_h , g_h and $d_h g_h$ figures of merit, which are calculated as 50 pCn^{-1} , $1.6 \times 10^{-3} \text{ Vm}^{-1} \text{ Pa}^{-1}$ and $80 \times 10^{-15} \text{ Pa}^{-1}$ respectively. A range of porous piezoelectric materials was manufactured using volatile species to generate the porosity. This process was chosen as it enabled a relatively large range of density (0.35–0.95) and porosity volume fraction to be manufactured and allowed direct comparison of properties at equivalent volume fraction,

but with a different microstructure and pore size. Polyethylene oxide, PEO, and poly(methyl methacrylate), PMMA, was used as a polymer in the BurPS process (burnt out polymer spheres). In addition to polymer volatile species, self-raising flour (SR) was also examined due to its finer particle size and an smaller pore size expected in the final microstructure.

The samples were manufactured by ball milling PZT-5H powder, water, PVA binder and the appropriate volatile additive in increasing weight fractions. After die pressing at 50 MPa, a heat treatment at 400 °C is employed, to burn off the additive, with further heating to 1125 °C for 2 h to sinter the ceramic. Sintering was undertaken under a lead oxide atmosphere to prevent lead loss from the PZT-5H. Changing the weight ratio of inclusion material (PMMA, PEO and SR) to PZT-5H ceramic powder modified the amount of porosity, measured by Archimedes method. After manufacturing the samples were electroded, corona poled and characterised after 24 h in terms of d_{33} and d_{31} using a Berlincourt PM25 Piezometer from Take Control. Permittivity (ϵ_{33}) was calculated by measuring the diameter (typically 12 mm) and thickness (typically 3mm) of the samples and measuring the sample capacitance using an Agilent Technology LCR at 1 kHz. The d_h , g_h and $d_h g_h$ parameters were calculated from the measured d_{33} , d_{31} and ϵ_{33} values and the equations discussed in the introduction. Microstructures were examined by optical microscopy.

3. Results and discussion

Fig. 1 shows typical optical micrographs of SR, PEO and PMMA porous materials at low and high porosities. The pore size is related to the size of the initial additive, with the pores size being typically 30–90 μm for SR, 70–200 μm for PEO and the largest pore sizes seen in the PMMA based samples (>250 μm). It is apparent that cracking exists in the PMMA samples which is perpendicular to the die pressing direction and the poling direction. This has been observed by previous workers and was thought to arise from the poling process.⁸ The cracks observed in this work are also present in unpoled samples and are more probably caused by the pressing forces which compress the ceramic powder more than the hard PMMA spheres. Upon releasing the pressing force, the powder expands and cracks are created in the sample perpendicular to the pressing direction. This was also reflected in the poor green strength of PMMA-based green bodies. The highest green strengths were obtained with the finer SF additive. It is interesting to note that as the porosity volume fraction increased there is increased connectivity between pores and the mean pore size increases (Fig. 1). This is often not considered in modelling although Levassort et al.

has considered 0–3 composites with mixed 3–3 connectivity.¹²

The longitudinal piezoelectric coefficient (d_{33}) as a function of density, shown in Fig. 2, reveals that as porosity is incorporated into the structure, there is a gradual decrease in d_{33} . At approximately 60% density, the d_{33} values are, however, still relatively large and are in excess of 300 pC N⁻¹. The transverse piezoelectric coefficient (d_{31}) as a function of density is shown in Fig. 3 which demonstrates that there is a more rapid decline in $-d_{31}$ with increasing porosity when compared to d_{33} . At approximately 60% density, $-d_{31}$ values are below 70 pC N⁻¹ and it is this rapid reduction in the transverse piezoelectric coefficient that leads to improved d_h coefficients. The mechanism for the process has been discussed in previous work.^{7,8}

For PMMA-based materials, higher d_{33} and smaller $-d_{31}$ values are achieved at the same density when compared to crack free PEO and SR. This may be due to presence of the cracks perpendicular to the poling

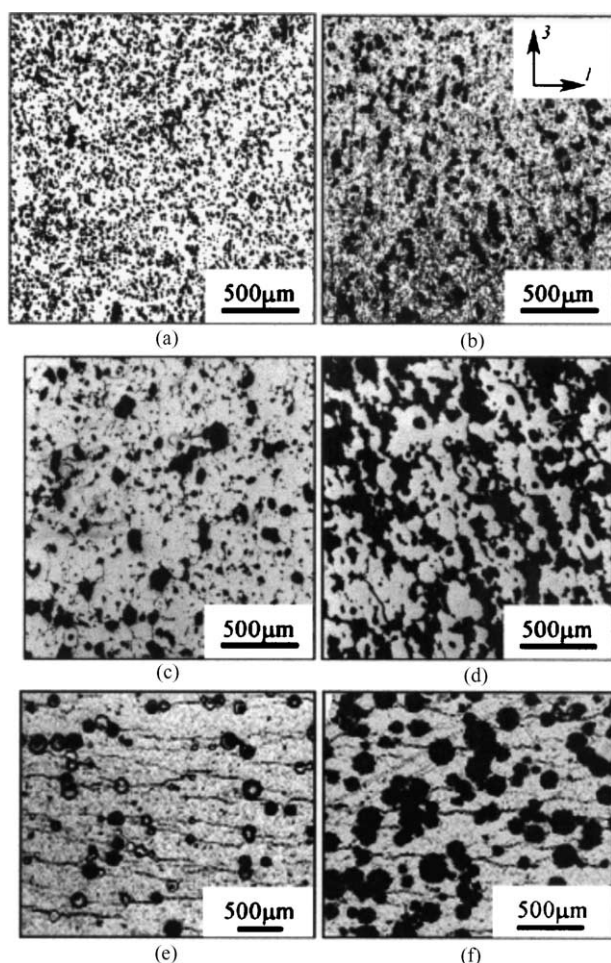


Fig. 1. Optical micrographs of porous piezoelectric materials. Poling is in the 3 direction as indicated: (a) SR low porosity, 28%, (b) SR high porosity, 50%, (c) PEO low porosity, (d) PEO high porosity, (e) PMMA low porosity, (f) cracks perpendicular to poling direction.

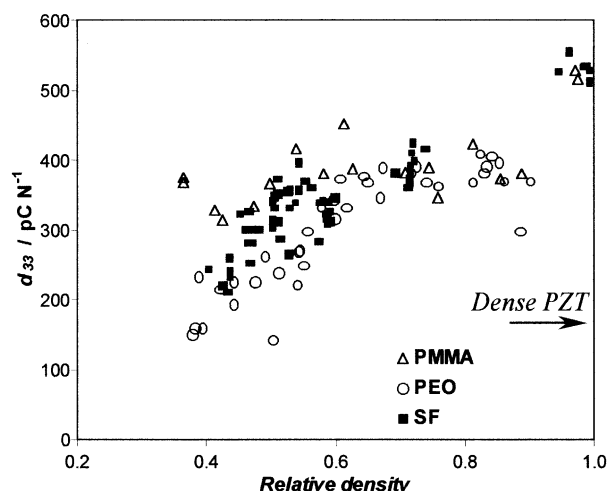


Fig. 2. Variation of longitudinal piezoelectric coefficient (d_{33}) with density. A gradual decrease in d_{33} with increasing porosity is observed.

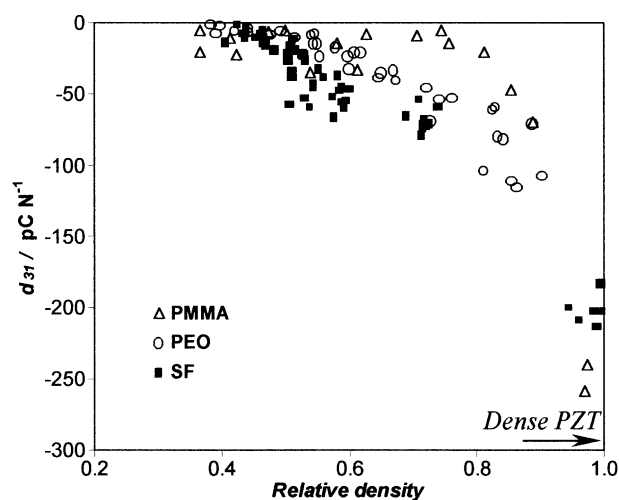


Fig. 3. Variation of transverse piezoelectric coefficient (d_{31}) with density. A rapid decrease in d_{31} with increasing porosity is observed.

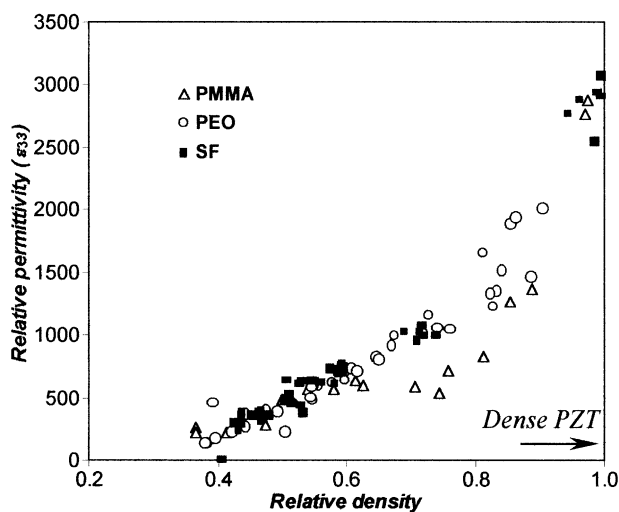


Fig. 4. Variation of longitudinal relative permittivity (ϵ_{33}) with density. As porosity replaces the high permittivity ceramic, ϵ_{33} decreases.

direction. During measurement of d_{33} using a Berlincourt piezometer, a small compressive force perpendicular to the crack direction (parallel to the poling direction) is applied which may act to close the cracks and reduce the effective porosity volume fraction. For d_{31} measurement, small compressive forces are applied parallel to the crack direction which can lead to crack opening and reduced d_{31} coefficients. This would imply high stress sensitivity in PMMA samples. When comparing the PEO and SR piezoelectric coefficients higher d_{33} and $-d_{31}$ are observed in the SR material which may be attributed to the smaller pore size of the SR and improved poling.

Fig. 4 shows that the permittivity (ϵ_{33}) of all the porous materials (PMMA, PEO and SR) decreases with increasing porosity, as would be expected. Similar permittivity values are observed for the PEO and SR samples as a function of density but PMMA based samples exhibit a lower permittivity, again due to the presence of cracks perpendicular to the measurement direction.

The reduced $-d_{31}$ coefficient and lower permittivity for the porous materials leads to an increase in hydrostatic voltage constant (g_h) and large improvements are observed when compared to dense PZT-5H, as seen in Fig. 5. While g_h for the PEO and SR based materials show a similar dependency with density, the lower permittivity for PMMA-based materials results in higher g_h values. The hydrostatic figure of merit ($d_h \cdot g_h$) as a function of density is shown in Fig. 6, which clearly demonstrates the large improvements in $d_h \cdot g_h$ possible by using porous materials when compared to dense PZT-5H. Although the cracks have a beneficial effect in this work and the PMMA additive produces the highest d_h , g_h and $d_h \cdot g_h$ figures of merit, the cracked microstructure can be undesirable in terms of strength,

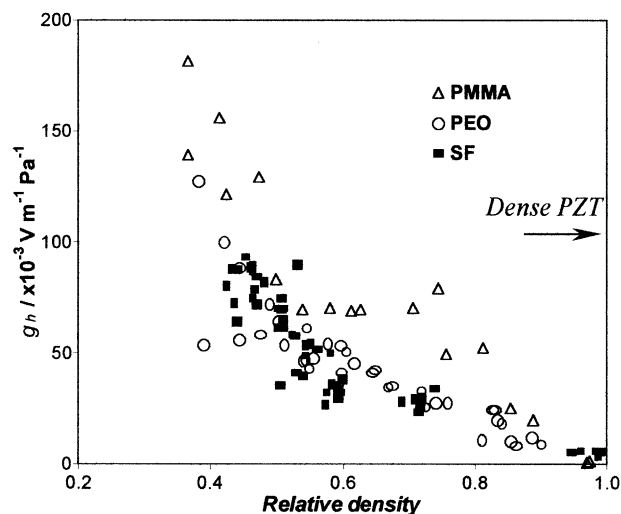


Fig. 5. Variation of hydrostatic voltage constant, $g_h = (d_{33} + 2d_{31})/\epsilon_{33}$, with density. The reduced $-d_{31}$ and ϵ_{33} leads to g_h increasing with porosity.

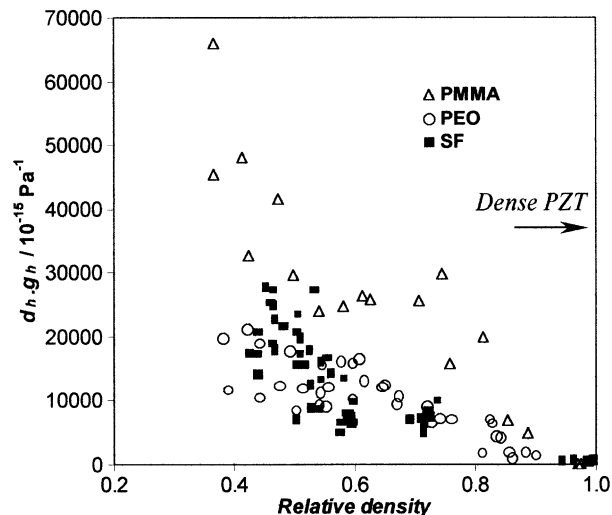


Fig. 6. Variation of hydrostatic figure of merit ($d_h \cdot g_h$) with density showing $d_h \cdot g_h$ increasing with porosity.

reliability and sensitivity of materials properties to hydrostatic pressures (depth sensitivity).

4. Conclusions

Porous piezoelectric materials have been manufactured over a range of density (40–95% theoretical) using different size volatile additives (PMMA, PEO and SR) and characterised in terms of d_{33} , d_{31} , ϵ_{33} and microstructure. For the range of density examined, an introduction of porosity leads to a decrease in $-d_{31}$ and ϵ_{33} , for all the materials, which results in improved g_h and $d_h \cdot g_h$ figures of merit when compared to dense PZT-5H. Examination of microstructures revealed cracking in PMMA-based porous ceramics due to lamination during pressing. The cracks, perpendicular to the pressing direction leads to a reduction in permittivity at the same porosity volume fraction when compared to the cracked free PEO and SR ceramics. The cracked microstructure was therefore observed to exhibit increased g_h and $d_h \cdot g_h$ figures of merit. The PMMA samples also had higher d_{33} and lower d_{31} for the same porosity volume fraction compared to PEO and SR, which is thought to be due to the cracked microstructure. While modelling research often considers 3–3 structures to have a specific pore size, morphology and connectivity, the microstructural observations revealed that the connectivity of pores and pore size increases with the degree of porosity.

For the PEO and SR samples studied, whose pore sizes were small in comparison to the size of sample, no significant differences in properties were observed even though they were of different pore size. This indicates that when attempting to optimise hydrostatic figures of

merit or porous materials, the ability to produce controlled volume fractions of porosity with homogeneous, defect free microstructures is more important than the ability to produce specific pore sizes.

Acknowledgements

The authors would like to thank EPSRC and Qinetiq for funding parts of this research.

References

1. Newnham, R. E., Skinner, D. P. and Cross, L. E., Connectivity and piezoelectric-pyroelectric composites. *Mater. Res. Bull.*, 1978, **13**, 525–536.
2. Geis, S., Fricke, J. and Lobmann, P., Electrical properties of PZT aerogels. *J. Euro. Ceram. Soc.*, 2002, **22**, 1155–1161.
3. Creedon, M. J. and Schulze, W. A., Axially distorted 3–3 piezoelectric composites for hydrophone applications. *Ferroelectrics*, 1994, **153**, 333–339.
4. Guillaussier, P. and Boucher, C. A., Porous lead zirconate titanate ceramics for hydrophones. *Ferroelectrics*, 1996, **187**, 121–128.
5. Marselli, S., Pavia, V., Galassi, C., Roncari, E., Craciun, F. and Guidarelli, G., Porous piezoelectric ceramic hydrophone. *J. Acoust. Soc. Am.*, 1999, **106**, 733–738.
6. Gallantree, H. R., Piezoelectric ceramic/polymer composites. *Brit. Ceram. Proc.*, 1989, **41**, 161–169.
7. Bowen, C. R., Perry, A., Kara, H. and Mahon, S. W., Analytical modelling of 3–3 piezoelectric composites. *J. Eur. Ceram. Soc.*, 2001, **21**, 1463–1467.
8. Rittenmyer, K., Shrout, T., Schulze, W. A. and Newnham, R. E., Piezoelectric 3–3 composites. *Ferroelectrics*, 1982, **41**, 189–195.
9. Craciun, F., Galassi, G., Roncari, E., Filippi, A. and Guidarelli, G., Electro-elastic properties of porous piezoelectric ceramics obtained by tape casting. *Ferroelectrics*, 1998, **205**, 49–57.
10. Hara, H., Perry, A., Stevens, R. and Bowen, C. R., Interpenetrating PZT/polymer composites for hydrophones. *Ferroelectrics*, 2002, **265**, 317–332.
11. Banno, H., Effects of shape and volume fraction of closed pores on dielectric, elastic and electromechanical properties of dielectric and piezoelectric ceramics—a theoretical approach. *Am. Ceram. Soc. Bull.*, 1987, **66**, 1332–1337.
12. Levassort, F. and Lethiecq, M., Effective electroelastic moduli of 3–3(0–3) piezocomposites. *IEEE Trans. Ultra. Ferro. Freq. Cntrl*, 1999, **46**, 1028–1034.